

Material Properties of the Dentate Maxilla

JILL PETERSON, QIAN WANG, AND PAUL C. DECHOW*

Department of Biomedical Sciences, Baylor College of Dentistry, Texas A&M University System Health Science Center, Dallas, Texas

ABSTRACT

The aim of this study was to determine regional variability of material properties in the dentate maxilla. Cortical samples were removed from 15 sites of 15 adult dentate fresh-frozen maxillas. Cortical thickness, density, elastic properties, and the direction of greatest stiffness were obtained. Results showed that cortical bone in the alveolar region tended to be thicker, less dense, and less stiff. Cortical bone from the body of the maxilla was thinner, denser, and stiffer. Palatal cortical bone was intermediate in some features but overall was more similar to cortical bone from the alveolar region. The principal axes of stiffness varied regionally. The regions with the greatest consistency were the alveolar area and the frontomaxillary pillar, where the grain of the cortical bone was aligned vertically from the incisors to the medial external aspect of the orbit. Elastic properties in the human maxilla, especially the orientation of the principal axes of stiffness, were more variable than in the mandible. Incorporation of these properties into finite-element models should improve their accuracy and reliability. *Anat Rec Part A*, 288A:962–972, 2006. © 2006 Wiley-Liss, Inc.

Key words: ultrasonic; cortical bone; biomechanics; function; finite-element modeling

In comparison to the mandible, understanding the biomechanics of the maxilla presents greater difficulties. The complexity of the maxilla results from the large number of sutures between the maxilla and bones contiguous with it and the sinuses that occupy almost the entire internal region of the body of the maxilla. The bone's unique gross morphology and shape allow for a variety of functions, including deglutition, respiration, and sensation (smell and sight), as well as serving as anchorage for a small portion of the masseter muscle. Due to this complexity, adaptation of the maxilla to function is not well understood.

The maxilla is comprised of several distinct anatomical regions, including the palate, nasal floor, alveolus, and body. Crossing these regions are structures or pillars that are interpreted as supports for biting and mastication including the zygomaticomaxillary pillar, the temporozygomatic pillar, and frontomaxillary pillar (Sicher and DuBrul, 1970).

Little is known experimentally about variability of the mechanical characteristics of the human dentate maxilla. In the monkey maxilla, patterns of bone strain suggest that significant loads are borne locally during mas-

tication and biting and that bone sutures and adjacent cavities buffer occlusal forces (Saijo and Sugimuro, 1993). As occlusal forces are dispersed at different tooth positions, maxillary surfaces bend outward away from the sinuses. Presumably, mechanical stimuli caused by mastication and biting are important in the maintenance of cortical bone structure in the maxilla and result in variations of function depending on location relative to different elements of the dentition and muscle attachments.

Grant sponsor: the National Institutes of Health, National Institute of Dental and Craniofacial Research (NIDCR); Grant number: K08 DE00403.

*Correspondence to: Paul C. Dechow, Department of Biomedical Sciences, Baylor College of Dentistry, 3302 Gaston Ave, Dallas, TX 75246. Fax: 214-828-8951. E-mail: pdechov@bcd.tamhsc.edu

Received 24 January 2006; Accepted 15 May 2006

DOI 10.1002/ar.a.20358

Published online 7 August 2006 in Wiley InterScience (www.interscience.wiley.com).

The sparse data on the material properties and related micromechanical features of maxillary cortical bone are further limited by a lack of consideration in the literature of its unique three-dimensional properties. The mechanical properties of the diaphyses of long bones are typically characterized along three axes, including the anatomical longitudinal axis, which is considered to be the axis of maximum stiffness. At right angles to the longitudinal axis are the circumferential axis, which parallels the plane of the cortical plate and is the least stiff direction in that plane, and the radial axis, which is perpendicular to the plane of the cortical plate and is the axis along which cortical thickness is measured.

In other craniofacial bones, the axis of maximum stiffness within the plane of the cortical plate does not necessarily coincide with anatomical axes. In human and baboon mandibles, it varies between anatomical regions (Schwartz-Dabney and Dechow, 2003; Wang and Dechow, 2004). In human skulls, at some sites in the mandible and most sites in the cranial vault and zygoma, axes within the plane of the cortical plate are not consistent between individuals (Peterson and Dechow, 2003). However, cortical bone in the rhesus monkey crania shows a high level of consistency among individuals (Wang and Dechow, 2006). In the maxilla, the axes of the maximum stiffness generally are oriented perpendicular to the alveolar border (Wang and Dechow, 2006). The orientation of the axes of stiffness in the cortical bone of the human maxilla is unknown, although it is reasonable to suggest that anatomical landmarks, as in the mandible and cranial vault, cannot determine these axes. The suggestion that grain in cortical bone, or the direction of maximum stiffness, aligns in the direction of maximum stress may be a reasonable conjecture to formulate hypotheses about material axes. However, little is known about the average orientations of maximum stresses in the human maxilla during the varied and complex patterns of loading during orofacial function.

Historically, the maxillary supports or pillars are thought to bear compressive stresses generated by occlusal forces along their longitudinal axes. Sicher and DuBrul (1970) theorize a three-pillared model (zygomaxillary, pterygomaxillary, and frontomaxillary), in which the pillars act as structural supports from the tooth row through the maxilla to the cranial vault to bear stresses generated by occlusal loads. We initially hypothesized that directions of maximum stiffness in maxillary cortical bone are oriented parallel to the long axes of these pillars.

While little is known about the material properties of cortical bone in the maxilla, some published data are available on bone density, although these studies primarily are radiographic and do not have true three-dimensional measurements of density. For example, Southard et al. (2000) show how the radiographic density of the maxillary alveolar process bone significantly declines with age in healthy dentate humans.

No systematic quantitative biomechanical analysis of the human maxilla exists, except some qualitative attempts (Sicher and DuBrul, 1970). Biomechanical modeling of zygomaticomaxillary complex is more difficult because there are a small number of active forces (i.e., bite force and muscle force) but a large number of possible reaction forces, in which their degree of interdependence is only poorly understood. Perhaps for this reason, force distribution along the bony zygomaticomaxillary complex in human

dentate patients has received little theoretical biomechanical analysis. Recently, finite-element analysis (FEA) has become a powerful tool in probing the interface between function and morphology, as it is able to estimate synchronous strain across an entire structure and enable interpretation of strain data from a global perspective (Richmond et al., 2005). We believed that the application of FEA in human facial skeletons would facilitate this study. Knowledge of elastic properties and its variation in the cortical bone of the human maxilla is indispensable for creating accurate finite-element models to explore the biomechanics and adaptation of the human face. Tests of model validity with or without the use of accurate elastic properties reveal that model precision can be substantially increased if accurate elastic properties are included in the model design (Strait et al., 2005).

Our goal is to explore the variability in the material properties of the cortical bone of the dentate maxilla. Our hypothesis is that there are important regional differences within the maxilla that correspond with variations in function and development.

MATERIALS AND METHODS

We used bone specimens removed from 15 dentate human crania selected from unembalmed, fresh-frozen whole cadaver heads. A random mix of subjects, seven females (48–95 years of age) and eight males (50–89 years of age) had a median age of 58.9 years. All specimens were Caucasian and were not collected from cadavers known to have died from primary bone diseases. All cadavers were from the willed body program at the University of Texas Southwestern Medical Center. Human tissue use conformed to all National Institutes of Health, state, and federal standards.

All crania were frozen shortly after death and were maintained in a fresh (unembalmed) condition. Crania were stored in freezers at -10°C prior to removal of bone specimens. The freezing process has been found to have a minimal effect on the elastic properties of the bone (Evans, 1973; Dechow and Huynh, 1996; Zioupos and Currey, 1998).

Cylindrical cortical bone specimens (4 mm in diameter) were harvested from maxillary sites located in three distinct regions: the palate (four sites), alveolar bone (four sites), and the body of the maxilla (seven sites; Fig. 1). Each cylinder of bone has a unique thickness that represents the cortical plate. Prior to removal, bone samples were marked with a graphite line that was parallel to the occlusal plane. This indicated the sample's orientation prior to removal. Trabecular bone was removed from the inner aspect of the cortical plate with a fine grinding wheel. The samples were stored in a solution of 95% ethanol and isotonic saline in equal proportions. This media maintains the elastic properties of cortical bone over time with minimal change (Ashman et al., 1984; Dechow and Huynh, 1996).

Each prepared bone specimen was measured using a digital caliper to determine the thickness of the bone cylinder. Sample weight and differential volume in water were used to calculate apparent density based on Archimedes' principle of buoyancy. Bone densities were required to calculate elastic properties from ultrasonic velocities. Each sample's physical properties were measured at least two times. If discrepancies were found,

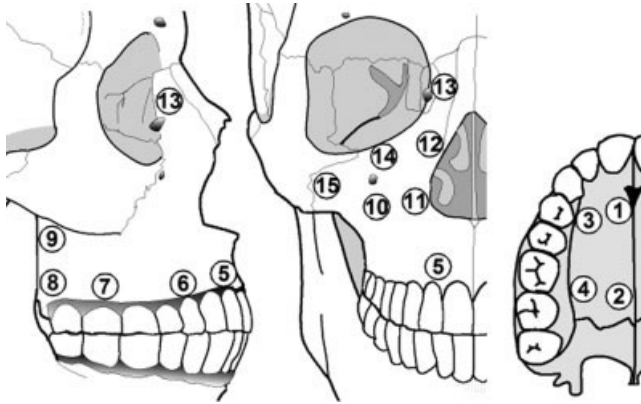


Fig. 1. Location of sites on the maxilla. Each site is numbered for reference.

measurements were repeated until consistent results were obtained.

Material property testing was performed using the pulse transmission technique previously described (Ashman, 1982, 1989; Ashman et al., 1984; Ashman and Van Buskirk, 1987). Specimen longitudinal velocities were measured in nine radial directions, as described in Schwartz-Dabney and Dechow (2003).

The direction of the axis of maximum stiffness or d_3 corresponded with the direction of peak ultrasonic velocity. We determined the axes of maximum stiffness by using a sine function fit of measurements of velocity at 22.5° intervals. Perpendicular to the axis of maximum stiffness within the plane of the cortical plate was the axis of minimum stiffness or d_2 . The velocity of the transverse waves was then measured with 5.0 MHz transducers (Panametrics V156-RM) along the three major axes d_1 (through the thickness of the cortical plate), d_2 , and d_3 , and in several off-axis orientations (Ashman et al., 1984).

Relationships between the various velocities through the specimen and their material properties were derived from the principles of linear elastic wave theory (Ashman et al., 1984). This theory, which is based on Hooke's law, allows computer generation of a 6×6 matrix of elastic coefficients, or C-matrix based on the time delay, width, and density of the bone samples. This matrix was used to calculate several elastic moduli as follows.

Elastic modulus (E): a measure of the ability of a structure to resist deformation in a given direction. Subscripts, as in E_1 , E_2 , or E_3 , indicate the orientation or axis for each elastic modulus. As mentioned above, the axis of E_3 , the elastic modulus in the direction of maximum stiffness in the cortical plane of the specimen, is perpendicular to that of E_2 , the elastic modulus in the direction of minimum stiffness in the cortical plane. The orientation of the axis of E_1 is perpendicular to the plane of the bone (and perpendicular to the E_2 and E_3), or through the thickness of the cortical plate.

Shear modulus (G): a measure of the stiffness in shear or angular deformation relative to applied shearing loads in a plane formed by the two axes indicated by the subscripts (G_{12} , G_{31} , or G_{32}).

Poisson's ratio (ν): a measure of the ability of a structure to resist deformation perpendicular to that of the

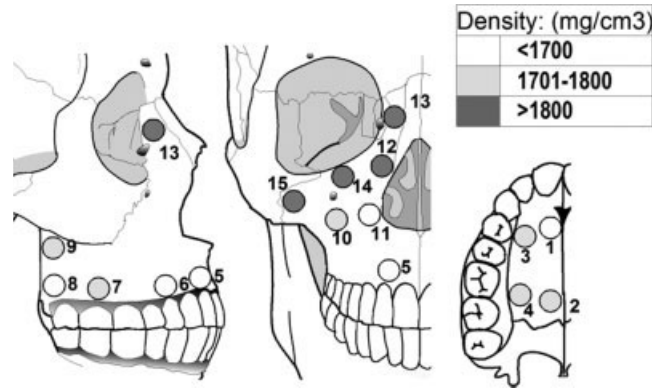


Fig. 2. The density of each site on the maxilla in three views is represented by shade.

applied load. The subscripts indicate orientation for Poisson's ratios in the same manner as in describing the shear moduli (ν_{12} , ν_{21} , ν_{13} , ν_{31} , ν_{23} , ν_{32}).

The elastic constants quantified the relationship between a load (stress) placed on a structure and the resulting deformation of that structure (strain), within its elastic range (Cowin and Hart, 1989; Dechow et al., 1993; Dechow and Hylander, 2000; Schwartz-Dabney and Dechow, 2003).

In addition to density, ash weights were determined for each bone sample. Wet bone samples were weighed, then dried at room temperature until the weight was constant for 48 hr. The bone samples were ashed in a muffle oven at 850°C for 12 hr. The ashed samples were reweighed and this weight was divided by the dry bone weight to determine a percentage ash weight (Barengolts et al., 1993; Nordsletten et al., 1994).

Data were stored in Microsoft Excel and analyzed using the Minitab statistical analysis program. Descriptive statistics, including means, standard deviations, and standard errors, were calculated for all measurements.

Assessment of differences between sites within the maxilla was restricted by the lack of independence between multiple samples taken from a single specimen. To test for differences thus required the use of an ANOVA with a repeated-measures design to account for the lack of independence (Zar, 1996; Peterson and Dechow, 2003). We used a balanced, unrestricted analysis of variance with a repeated measures design and subject as the random factor to test for overall differences in density, cortical thickness, and elastic properties.

Circular data analysis was used to describe the orientations of maximum stiffness and to test differences between sites. Circular descriptive statistics including mean vector, circular standard deviation, standard error, confidence intervals, and a Rayleigh's test of uniformity (Zar, 1999) were calculated with the Oriana Statistical Analysis Program.

RESULTS

Overall, there were significant differences between sites in thickness and density that discretely outlined regions of the maxilla (Figs. 2 and 3, Table 1). The pala-

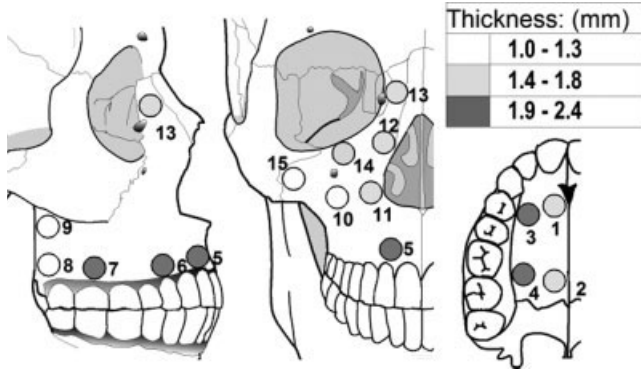


Fig. 3. Thickness of each site on the maxilla in three views is represented by shade.

TABLE 1. Density (unit: mg/cm³), cortical thickness (unit: mm) and ash weight

Site	N	Density		Thickness		Ash weight	
		Mean	SD	Mean	Mean	%	Mean
1	12	1.65	0.17	1.7	0.5	56	5
2	10	1.75	0.14	1.8	0.9	55	9
3	11	1.75	0.18	2.3	1.1	57	5
4	10	1.70	0.16	2.0	1.0	53	7
5	14	1.65	0.15	2.2	1.3	57	5
6	8	1.64	0.19	2.4	1.6	58	9
7	11	1.72	0.20	2.1	0.9	54	11
8	6	1.61	0.14	1.2	0.6	54	15
9	6	1.77	0.16	1.0	0.3	53	15
10	10	1.75	0.16	1.2	0.5	56	8
11	9	1.69	0.15	1.7	0.7	54	11
12	11	1.82	0.12	1.5	0.4	53	12
13	11	1.83	0.17	1.4	0.3	50	13
14	11	1.81	0.11	1.5	0.6	55	7
15	7	1.90	0.12	1.1	0.3	61	5
Grand mean		1.75	0.16	1.9	0.9	56	9
ANOVA		F	F	P	F	P	F
Sites		4.7	0.001	5.4	0.001	NS	NS

tal site 3 and the alveolar sites supporting the teeth tended to be thicker than the other maxillary sites. The thickest sites were buccally and lingually near the canine (site 3: 2.3 mm; site 6: 2.4 mm). The thinnest sites were found at the pterygomaxillary process, site 9 (1.0 mm) and site 8 (1.2 mm), and at the area close to the zygomaticomaxillary suture, site 15 (1.1 mm) and site 10 (1.2 mm).

Density showed similar results to that of thickness, yet in a different regional pattern. Overall, where cortical bone was thin, its density was high. For instance, the infraorbital sites (12–15) on the body of the maxilla (Fig. 4) ranged in thickness from 1.1 to 1.5 mm, yet were high in density (>1.80 g/cm³). Overall, the densest site 15 (1.90 g/cm³) was at the zygomaticomaxillary suture, where the high density contrasted with the thinness of the cortex (1.1 mm; Table 1). Sites 5, 6, and 7 followed this trend with thicknesses ranging from 2.1 to 2.4 mm, yet density ranged from 1.64 to 1.75 g/cm³. However, there were some exceptions. For example, site 8 had the least dense (1.61 cm³) and very thin (1.2 mm) cortical bone.

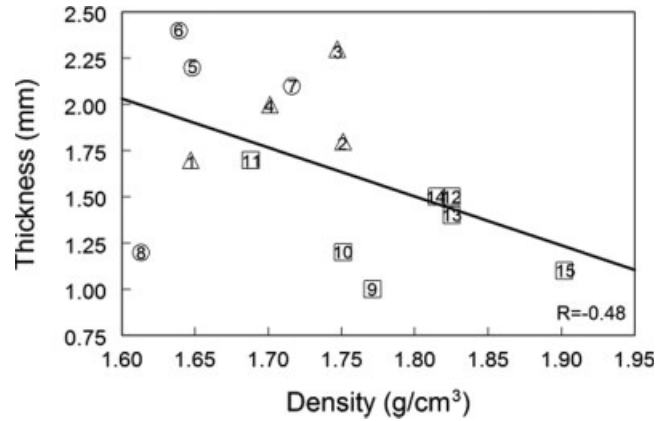


Fig. 4. Scatter plot of thickness vs. density. Each site is numbered. Circles represent alveolar bone sites, triangles are used for palatal sites, squares are used for sites located on the body of the maxilla. There is a significant relationship ($R = -0.48$; $P < 0.001$) showing that as thickness decreases density increases.

There were no significant differences between sites in ash weight (Table 1). There was no correlation between cortical density and ash weight, except that site 15 had both the highest ash weight (61%) and density.

The values for elastic moduli demonstrated differences by direction, in that E_3 was larger than E_2 , which was larger than E_1 (Fig. 5, Table 2). There were significant differences between sites for E_2 and E_3 (Fig. 5, Table 2), yet E_3 showed much greater values. For instance, site 3 was the stiffest site on the palate and had the highest E_3 (17.3 GPa), which was higher than that of site 5 near the incisor on the buccal cortical plate (14.3 GPa). Yet the stiffest site tested overall was site 15 at the zygomaticomaxillary suture (18.7 GPa). Less stiff sites included 12, 13, and 14 (17.0–17.8 GPa) on or near the piriform process; they were also thin (1.4–1.5 mm) and yet very dense (1.81–1.83/cm³). The elastic moduli at the pterygomaxillary site 8 were the smallest (E_1 : 6.9 GPa; E_2 : 8.8 GPa; E_3 : 10.5 GPa). Yet site 9, which is superior to site 8, was exceptionally higher in elastic moduli (E_1 : 9.8 GPa; E_2 : 11.7 GPa; E_3 : 15.6 GPa) in comparison. E_3 tended to be greater near sutures such as the frontomaxillary (site 13) and zygomaticomaxillary (site 15) sutures. These sites also had a greater density (Fig. 3, Table 1). Yet the midpalatal sutural sites (1 and 2) had relatively low density and stiffness.

For the ratio of E_2/E_3 , the majority of sites within the dentate maxilla were moderately anisotropic with ratios ranging from 0.69 to 0.85 (Figs. 6 and 7, Table 3). There were significant differences between the sites for anisotropy and the sites tended to cluster regionally. Site 11 near the piriform process had the highest anisotropy (0.69). Sites with less anisotropy were 2 and 4 on the palate, and 6 and 7 on the alveolar region. Site 8 on the alveolar region, where the lowest elastic moduli were measured, had the least anisotropy (0.85). The sites in the region of the infraorbit were moderately anisotropic.

Like elastic moduli, the values for shear moduli demonstrated differences by direction, in that G_{23} was larger than G_{31} , which was larger than G_{12} (Fig. 8, Table 4). There was a significant difference between sites for shear moduli (Fig. 8, Table 4). There were increased

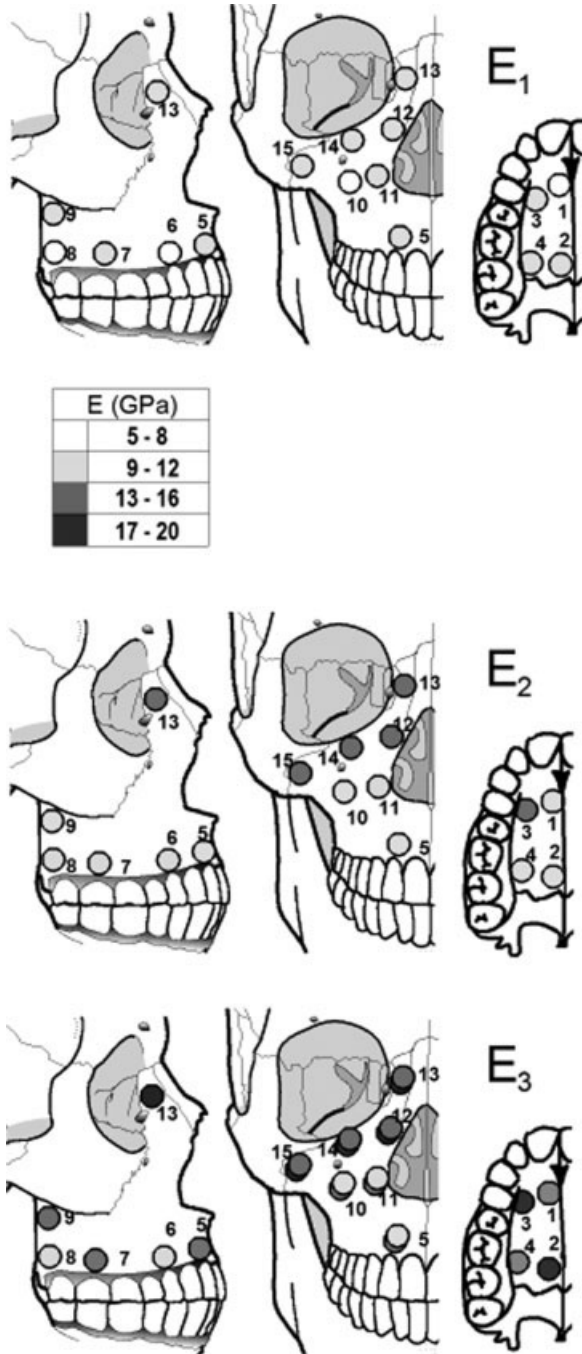


Fig. 5. Elastic moduli at each site in three views are represented by shade.

shear moduli at site 15 near the zygomaticomaxillary suture and at infraorbital sites 12 and 14 (Table 4) compared to the other sites ($G_{23} > 6.0$ GPa). Site 3 on the palate nearest to the canine showed the greatest shear moduli (G_{12} : 4.1 GPa; G_{23} : 4.5 GPa; G_{33} : 5.9 GPa) compared to the other palatal sites. As for elastic moduli, pterygomaxillary site 8 showed lower shear moduli compared to site 9.

Poisson's ratios (Fig. 9, Table 5) showed significant directional differences. The highest Poisson's ratio were

TABLE 2. Elastic moduli (unit: GPa)

Site	E ₁		E ₂		E ₃	
	Mean	SD	Mean	SD	Mean	SD
1	8.3	1.9	11.3	2.7	14.1	2.9
2	8.9	1.9	11.9	2.3	16.5	4.0
3	10.3	2.0	13.6	2.1	17.3	3.4
4	8.9	2.9	10.9	2.7	15.6	3.7
5	10.0	3.3	11.0	2.7	14.3	3.8
6	7.2	1.5	8.7	2.3	12.2	1.9
7	9.8	2.4	11.3	3.0	16.0	4.3
8	6.9	1.1	8.8	1.0	10.5	1.3
9	9.8	2.3	11.7	1.4	15.6	2.8
10	7.6	2.3	10.7	3.3	14.2	4.2
11	9.0	1.9	11.2	2.2	16.4	3.6
12	10.0	1.7	13.5	1.6	17.6	3.4
13	9.9	3.0	12.8	2.8	17.0	3.3
14	9.4	1.6	13.3	2.1	17.8	2.3
15	9.2	1.5	14.0	1.7	18.7	3.4
Grand mean	9.1	2.3	11.7	2.7	15.6	3.7
ANOVA	F	P	F	P	F	P
Sites	1.51	NS	3.02	0.001	3.87	0.001

Note: Sample size in this and following tables is the same as in Table 1.

V_{31} and V_{23} (>0.49), and the smallest Poisson's ratios were V_{21} and V_{32} (<0.30). There were no significant differences between sites for each ratio, but some showed regional differences. For example, V_{21} showed a distinct pattern in that the infraorbital area had lower values than that of any other area, while V_{23} had a relatively high value in this area.

Rayleigh's test for uniformity demonstrated significant mean directions ($P \leq 0.05$) of the maximum stiffness (E_3) in seven sites, including sites 5-7 in the alveolar area, 11 and 12 in the frontomaxillary pillar, and 1 in the palatal area (Fig. 10, Table 6). Sites 4, 10, and 13 also had significant mean directions ($0.05 < P \leq 0.072$). Six sites on the external maxillary surface showed a distinct pattern in that the direction of stiffness (Fig. 10) was perpendicular to the long axis of the frontomaxillary suture.

DISCUSSION

Overall, the material property results define regions of the maxilla. Cortical bone in the alveolar region tends to be thicker, less dense, and less stiff. Cortical bone from the body of the maxilla is thinner, denser, and stiffer. Palatal cortical bone is intermediate in some features but overall is more similar to cortical bone from the alveolar region. The principal axes of stiffness varied regionally and were not as consistent as those in the mandible (Schwartz-Dabney and Dechow, 2003). The regions with the greatest consistency were the alveolar area and the frontomaxillary pillar, where the grain of the cortical bone was aligned vertically from the incisors to the medial external aspect of the orbit. A similar pattern is also observed in rhesus monkey crania (Wang and Dechow, 2006). Cortical bones near the incisors and canines (sites 3, 5, and 6) has greater thickness than at other maxillary alveolar sites, but its density and stiffness are intermediate. This sampling region is at the interface between the anterior dentition and base of the frontomaxillary pillar and anterior palate, where the peak of a strain gradient is found during incisal biting in

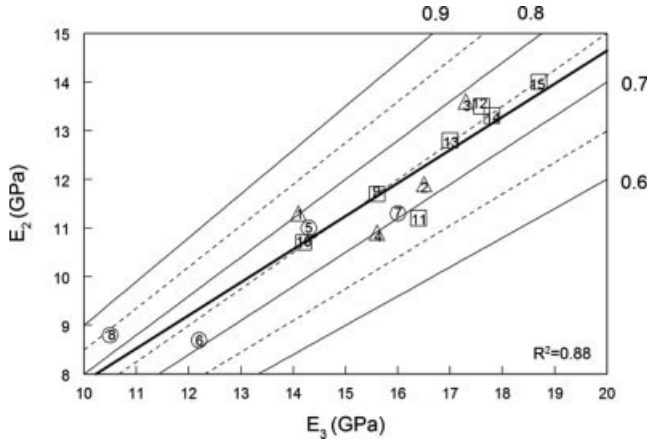


Fig. 6. Scatter plot of E_2 vs. E_3 or anisotropy. E_2 is the elastic modulus in the direction of minimum stiffness in the cortical plane and E_3 is the elastic modulus in the direction of maximum stiffness. There is a significant relationship ($R = 0.94$; $P < 0.001$) showing that as E_2 increases, so does E_3 .

TABLE 3. Anisotropy

Site	Anisotropy	
	Mean	SD
1	0.81	0.11
2	0.74	0.11
3	0.80	0.10
4	0.70	0.09
5	0.78	0.09
6	0.72	0.17
7	0.72	0.13
8	0.85	0.07
9	0.77	0.11
10	0.77	0.12
11	0.69	0.08
12	0.78	0.10
13	0.75	0.08
14	0.75	0.11
15	0.77	0.15
Grand mean	0.76	0.11
ANOVA	F	P
Sites	2.15	0.018

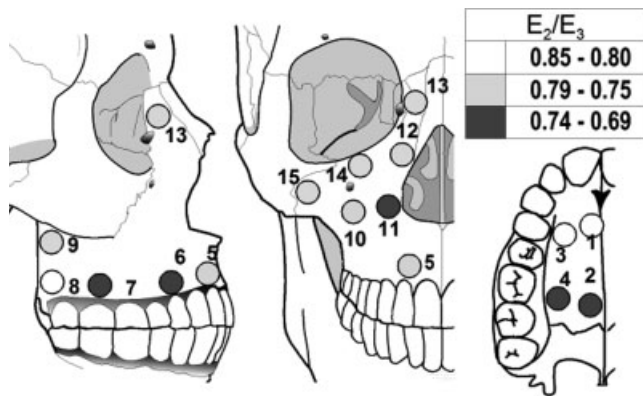


Fig. 7. Anisotropy for the maxilla in three views is represented by shade.

monkeys (Hylander, 1987). The thick cortical bone here is likely important as a functional adaptation.

Site 7 above M^2 and under the root of the zygomatic process has the densest and stiffest cortical bone in the alveolar area. This is not surprising, as we might expect higher loads in this area due to the mechanical advantage of the muscles of mastication that results in larger occlusal forces in this area.

The overall structure of the alveolus in the maxilla is similar to cranial bone in that it has a buccal cortical plate, a palatal cortical plate, and trabecular bone sandwiched between the two. Wherever a tooth crypt resides, there exists a circumferential cortical plate or lamina dura that interfaces with the periodontal ligament attaching to the tooth. The posterior dentition is distinguished by a broader region of alveolar bone and increased lamina dura because the molars are wider and have multiple roots compared to the narrower alveolar bone and tooth roots associated with the anterior dentition. The broader alveolar ridge posteriorly is able to maintain a greater volume of trabecular structures and lamina dura to support the tooth roots. This

contrasts with the anterior dentition, where greater loads are borne by the external cortical bone adjacent to the single roots of the teeth. Thus, we might expect adaptations, such as greater thickness, density, and stiffness, for bearing more concentrated loads in the cortical bone surrounding the anterior dentition, and indeed in this study we do find thicker bone in the anterior alveolar region and the palatal sites closest to the teeth, which might be the most effective way to resist the loads induced by biting and mastication.

The functional combination of a thin cortical plate overlying an extensive internal trabecular network is well understood in areas of the postcranial skeleton, such as the vertebral bodies and the proximal and distal regions of long bones. In these regions, this combination distributes load over a broader region. This pattern is found in the facial skeleton, not only in the alveolus of the maxillary molars as discussed above, but also in the zygomatic bone and the body of the maxilla, where the cortical bone is thinner (Bromage, 1992).

The maxilla has similar patterns of anisotropy as that found in the mandible, in which Schwartz-Dabney and Dechow (2003) found E_2 to be intermediate between E_1 and E_3 . However, overall anisotropy in the maxilla tends to be smaller than in the mandible. This is unlike the cranial vault in which E_1 and E_2 are often similar and less in magnitude than E_3 (Peterson and Dechow, 2003). The cranial vault is unusual in this regard in that elastic properties superficially resemble the transverse isotropy of postcranial long bones (Katz and Meunier, 1987; Cowin and Hart, 1989; Weiner et al., 1999; Wirtz et al., 2000).

There is a bony fusion between the lateral and medial pterygoid plates and the pterygomaxillary process. Bending of the midface during biting could result in a stress concentration in the maxilla near this region of bony fusion. It is interesting that site 9, nearest the fusion of the maxilla and pterygoid process, is on average much stiffer (15.6 vs. 10.5 GPa) than site 8 on the maxillary tuberosity, which is more distant from the fusion and is located near the molars. This may indicate an adaptation for resistance to stress due to bending in this region at or near site 9.

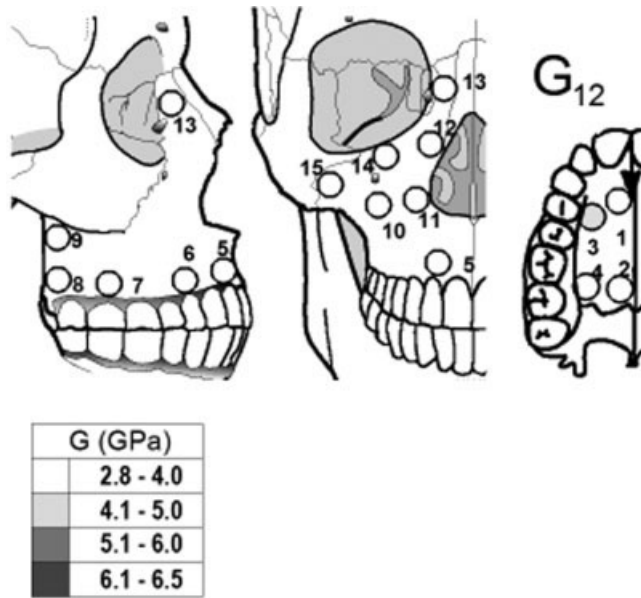


TABLE 4. Shear moduli (unit: GPa)

Site	G ₁₂		G ₃₁		G ₂₃	
	Mean	SD	Mean	SD	Mean	SD
1	3.4	0.9	3.7	0.7	4.9	1.2
2	3.6	0.8	4.1	0.8	5.4	1.0
3	4.1	0.6	4.5	1.0	5.9	1.1
4	3.5	1.2	4.0	1.0	5.1	1.1
5	3.8	1.2	4.2	1.3	4.9	1.4
6	2.8	0.8	3.5	0.4	4.2	0.9
7	3.7	1.0	4.5	1.1	5.2	1.2
8	2.8	0.3	2.9	0.3	4.0	0.7
9	3.6	0.7	4.4	1.0	5.6	1.0
10	3.1	0.8	3.5	1.0	5.3	1.5
11	3.5	0.7	4.1	0.8	5.3	0.9
12	4.0	0.6	4.5	0.7	6.2	0.7
13	4.0	1.1	4.4	1.2	5.9	1.1
14	3.9	0.7	4.4	0.8	6.1	0.9
15	3.8	0.8	4.3	0.5	6.5	0.7
Grand mean	3.6	0.9	4.1	1.0	5.4	1.2
ANOVA	F	P	F	P	F	P
Sites	1.90	0.040	2.08	0.023	2.66	0.003

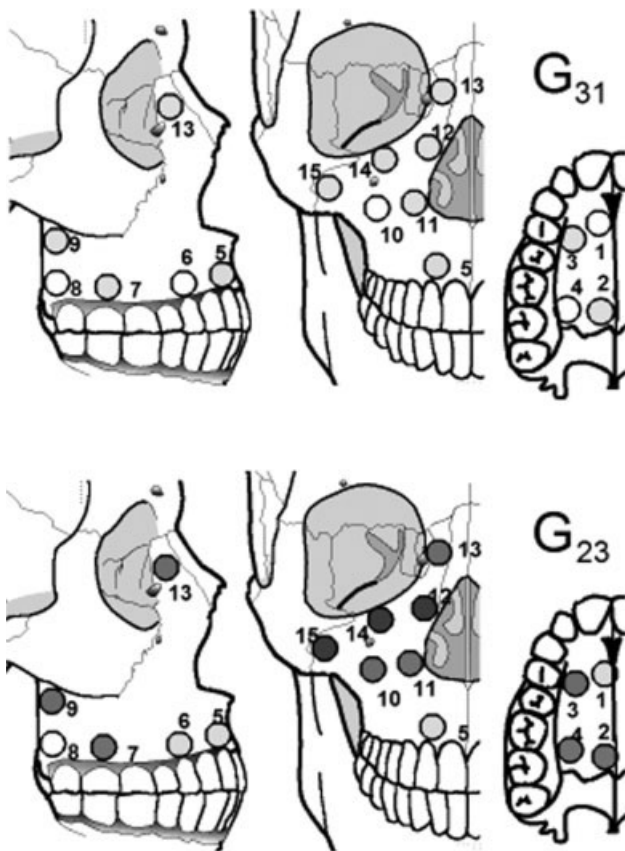


Fig. 8. Shear moduli at each site in three views are represented by shade.

Peterson and Dechow (2003) show that muscle-bearing cortical bone in the cranial vault tends to be stiffest in the direction of d_3 . There are few muscle-bearing cortical regions in the maxilla, but one site (15) close to the

anteriormost portion of the masseter muscle attachment had some of the highest values of E_3 , similar to areas on the parietal bone directly adjacent to attachments of the temporalis muscle.

Qualitative biomechanical analysis of the midface by Sicher and DuBrul (1970) suggests that the frontomaxillary and zygomaticofrontal pillars of bone buttress and transmit bite force during masticatory activities. Three of the sites with significant orientations in the dentate maxilla (5, 11, and 12) are located lateral to the piriform process on the frontomaxillary pillar (site 13 in this area has a similar and significant mean direction). Endo (1966) found a higher magnitude of compressive strain at the frontomaxillary pillar of bone during incisal biting compared to molar biting. He concludes that intensive strains appear at the alveolar process and body of the maxilla near the loaded tooth, the lower part of the lateral margin of the orbit, and the inferolateral corner of the orbit and its vicinity.

Other regions of cortical bone that show significant mean directions of stiffness on both the palatal and buccal surfaces are located near the first molars (sites 6 and 7), although these sites show different directions of stiffness between buccal and lingual aspects. The axis at site 4 is perpendicular to the tooth axis as at site 1, while at sites 5–7 the mean axis is parallel to it. The common direction suggests a possible uniform direction of strain in the bone during the most common functions (biting). Orientation of maximum stiffness at sites 5–7 might reflect the vertical direction of the maximum strain in this region during masticatory function. However, the functional significance of the difference between buccal and lingual aspects, as well as the lack of a significant orientation at other alveolar and palatal sites, is unclear.

Schwartz-Dabney and Dechow (2003) find that in almost all alveolar cortical regions of the mandible, the axes of the maximum stiffness have uniform orientations among specimens. Lingually, these orientations are perpendicular to the tooth axis, as at site 1 in the palate. Buccally, they are in more of an anteroinferior-posterosuperior orientation. In the mandible, the orientations in the alveolar regions resemble that of cortical



Fig. 9. Poisson's ratios at each site in three views are represented by shade.

bone found throughout the corpus. The maxilla sustains similar occlusal loads as the mandible and it is likely to have similar magnitudes of bone strain. Thus, we expected to find consistent patterns of orientation of the axes of maximal stiffness throughout the maxilla. However, significant orientations were found at only 7 of 15 sites, which tended to have greater variability in orientation than most sites in the mandible.

The three-dimensional intermediate structure of cortical bone in the craniofacial skeleton is not well documented. Presumably, osteonal structure and direction contribute to variations in directions of maximum stiffness in the cortical plate. The only historic studies to address this issue used the split-line technique. Split lines reflect aspects of bone histology including osteon structure and vascular canal orientation (Seipel, 1948; Tappen, 1954, 1957; Dempster and Coleman, 1960; Buckland-Wright, 1977). In com-

paring past split-line analyses (Seipel, 1948; Tappen, 1953) to our results for maximum direction of stiffness, there is an apparent correlation in some regions but not in others. Tappen (1953) states that at the alveolar bone margin, the split lines are perpendicular to the tooth roots on both the lingual and buccal surfaces. Superior to the margin near the apices of the teeth, the split lines parallel the tooth roots. Our cortical specimens in the buccal alveolar region show a parallel pattern to the tooth roots. However, on the lingual, alveolar sites show a perpendicular orientation of maximum stiffness to the tooth root except at site 8. Together with other features, such as the thinnest, least dense, and least stiff cortical bone, the area around site 8 might bear weak occlusal loads, corresponding to the diminished functional significance of M³.

One problem in attempting to compare our directions of maximum stiffness with split-line orientations is that

TABLE 5. Grand means of Poisson's ratios

Site	V ₁₂		V ₁₃		V ₂₁		V ₂₃		V ₃₁		V ₃₂	
	Mean	SD	Mean	SD	Mean	SD	Mean	SD	Mean	SD	Mean	SD
1	0.34	0.08	0.29	0.07	0.25	0.08	0.47	0.13	0.50	0.12	0.32	0.10
2	0.37	0.06	0.28	0.07	0.22	0.06	0.51	0.11	0.52	0.08	0.3	0.07
3	0.37	0.08	0.30	0.09	0.25	0.07	0.48	0.07	0.50	0.16	0.31	0.08
4	0.41	0.09	0.30	0.07	0.20	0.09	0.51	0.14	0.53	0.10	0.28	0.12
5	0.37	0.10	0.33	0.09	0.23	0.11	0.41	0.10	0.48	0.16	0.29	0.13
6	0.42	0.18	0.29	0.10	0.21	0.15	0.50	0.22	0.5	0.17	0.27	0.19
7	0.42	0.13	0.28	0.08	0.22	0.09	0.48	0.14	0.47	0.17	0.31	0.15
8	0.38	0.07	0.36	0.12	0.18	0.11	0.5	0.15	0.56	0.20	0.22	0.13
9	0.43	0.15	0.3	0.04	0.19	0.10	0.53	0.17	0.51	0.15	0.24	0.09
10	0.38	0.11	0.34	0.07	0.13	0.07	0.56	0.21	0.63	0.13	0.17	0.10
11	0.4	0.09	0.29	0.13	0.19	0.09	0.49	0.10	0.5	0.18	0.28	0.16
12	0.38	0.02	0.32	0.07	0.18	0.06	0.52	0.08	0.55	0.09	0.25	0.10
13	0.38	0.09	0.31	0.04	0.19	0.08	0.51	0.16	0.56	0.12	0.25	0.10
14	0.35	0.10	0.27	0.10	0.22	0.10	0.51	0.16	0.51	0.20	0.29	0.14
15	0.38	0.08	0.28	0.07	0.19	0.09	0.58	0.15	0.57	0.16	0.24	0.09
Grand mean	0.38	0.1	0.3	0.08	0.21	0.09	0.49	0.14	0.51	0.15	0.28	0.12
ANOVA	F	P	F	P	F	P	F	P	F	P	F	P
Sites	1.4	NS	0.53	NS	1.29	NS	1.17	NS	1.46	NS	1.74	NS

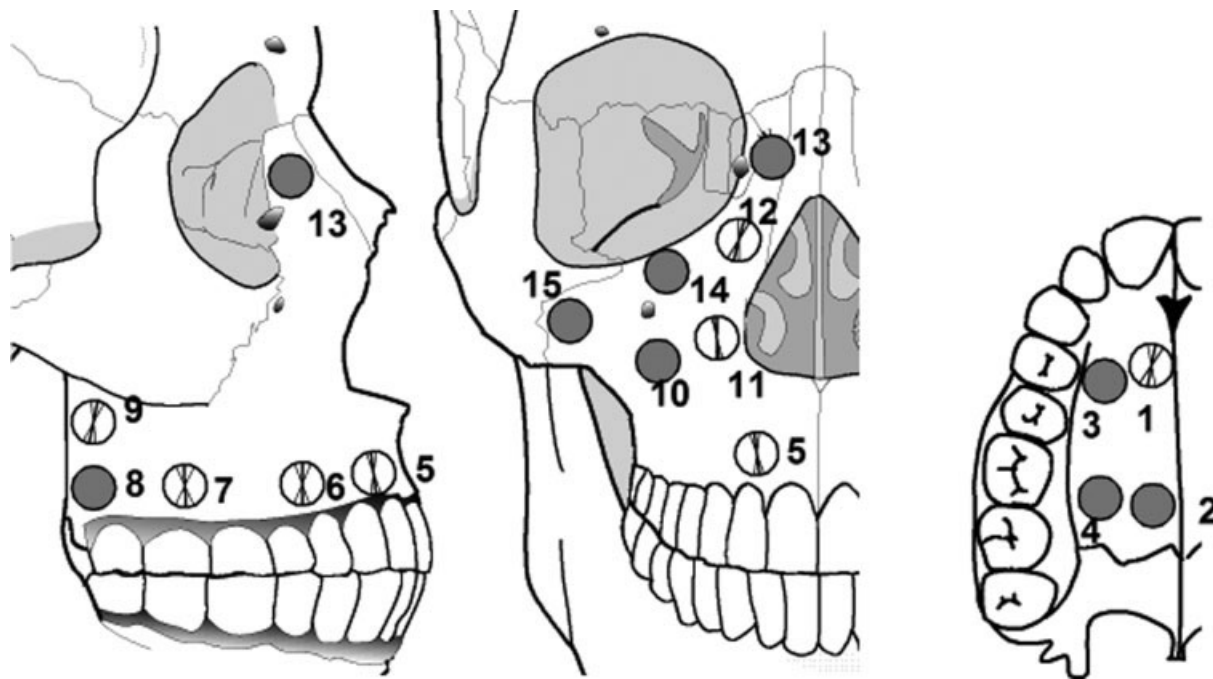


Fig. 10. Orientation of axes of maximum stiffness in the maxilla in three views. Seven sites show significant mean orientations of the axis of maximum stiffness as indicated by the bold line at each site. This line designates the mean orientation and the nonbold lines on either side of the orientation line are the 95% confidence intervals. All shaded sites without orientation lines have no significant maximum direction of stiffness.

the literature does not document variability in split lines quantitatively. In the mandible, Schwartz-Dabney and Dechow (2003) found that split lines on the whole correspond with directions of maximum stiffness. In the cranium and zygoma, correspondence between the two is at best sporadic (Peterson and Dechow, 2003). Tappen (1953) reiterates that split-line patterns of the human face show variability in extent and degree of organiza-

tion in different regions but he did not quantify the variation. Based on strain gage studies, Endo (1966) concurs that the principal strain axes found in the human facial skeleton seem to be similar to some degree to the orientation of the split lines. Endo (1966) states that these results may be coincidental at best.

Material properties of cortical bone are also important for interpreting bone strain and for creating accurate fi-

TABLE 6. Direction of greatest stiffness by degrees

Site	Mean vector	Circular CI	Rayleigh's test of uniformity ^a
	Mean°	95% CI	P value
1	168.6	34.1	0.04
4	165.9	34.5	0.072
5	6.7	23.9	0.002
6	178.5	33.3	0.031
7	2.1	34.2	0.041
9	168.5	26.8	0.012
10	178.5	35.8	0.063
11	5.4	15.7	<0.001
12	165.5	28.1	0.005
13	1.2	36.1	0.068

^aOriana indicated the above sites as significant using Rayleigh's test of uniformity or test of significance.

nite-element models in studies of bone deformation in response to stress (Dechow and Hylander, 2000; Richmond et al., 2005; Strait et al., 2005). Schwartz-Dabney and Dechow (2003) conclude that regions of cortical bone with greater anisotropy and greater variation in the direction of maximum stiffness result in larger errors in calculating stresses from measured bone strains, or strains from predefined loads in finite-element models. They show that variations in anisotropy and the orientations of maximum stiffness in the mandible are sufficiently small in most cortical regions to make reasonable estimates, if the average values of elastic properties are used in the calculations. A study of the cranial vault concluded that errors in calculating stresses from measured bone strains are likely to be larger because of the variations in orientation and anisotropy (Peterson and Dechow, 2003). In the maxilla, these errors are also likely to be larger at many sites because of the lack of a consistent orientation, even though the variation in the degree of anisotropy is relatively small.

Overall, little is known about theoretical mechanics of the midface and palate during function either in humans or in animal models. No systematic biomechanical analyses of the midface are available in the literature, though in vivo strain studies demonstrate that most regions of the midface and palate bear significant loads during function in vertebrate skulls (Hylander et al., 1991; Ross, 2001; Ravosa et al., 2002; Wang et al., 2006). Theoretically, the active forces can be experimentally measured or estimated, as can the bite force, so only the joint reaction forces must be solved for numerically. Biomechanical modeling of the zygomaticomaxillary complex is more difficult because there are a small number of active forces (i.e., bite force and muscle force) but a large number of possible reaction forces and their degree of interdependence is only poorly understood. Perhaps for this reason, force distribution along the bony zygomaticomaxillary complex in dentate humans has received little theoretical biomechanical analysis. In order to explore the link between stress patterns and bone material properties (intrinsic feature of bone), the structural properties, which are the extrinsic feature of the skeleton, should be considered, which include the bone mass, bone material properties, organization of cortical and trabecular bone, and the loading regime. Armed with the material properties of human maxillae in this study, finite-element models could be developed, which will

provide a firmer basis to explore the relationship of stress patterns to bone material properties in the midfacial skeleton.

LITERATURE CITED

- Ashman RB. 1982. Ultrasonic determination of the elastic properties of cortical bone: techniques and limitations. PhD dissertation. Tulane University, New Orleans, LA.
- Ashman RB, Cowin SC, Van Buskirk WC, Rice JC. 1984. A continuous wave technique for measurement of the elastic properties of cortical bone. *J Biomech* 17:349–361.
- Ashman RB, van Buskirk WC. 1987. The elastic properties of a human mandible. *Adv Dent Res* 1:64–67.
- Ashman RB. 1989. Experimental techniques. In: Cowin SC, editor. *Bone mechanics*. Boca Raton, FL: CRC Press. p 76–95.
- Barengolts EI, Curry DJ, Bapna MS, Kukreja SC. 1993. Effects of endurance exercise on bone mass and mechanical properties in intact and ovariectomized rats. *J Bone Miner Res* 8:937–942.
- Bromage TG. 1992. Microstructural organization and biomechanics of the macaque circumorbital region. In: Smith P, Tchernov E, editors. *Structure, function and evolution of teeth*. London: Freund Publishing House. p 257–272.
- Buckland-Wright JC. 1977. Microradiographic and histological examination of the split-line formation in bone. *J Anat* 124:193–203.
- Cowin SC, Hart RT. 1989. Errors in the orientation of the principal stress axes if bone tissue is modeled as isotropic. *J Biomech* 23:349–352.
- Dechow PC, Nail GA, Schwartz-Dabney CL, Ashman RB. 1993. Elastic properties of human supraorbital and mandibular bone. *Am J Phys Anthropol* 90:291–306.
- Dechow PC, Huynh T. 1996. Elastic properties and biomechanics of the baboon mandible. *Am J Phys Anthropol* 22(Suppl):94–95.
- Dechow PC, Hylander WL. 2000. Elastic properties and masticatory bone stress in the macaque mandible. *Am J Phys Anthropol* 112:553–574.
- Dempster WT, Coleman R. 1960. Tensile strength of bone along and across the grain. *J Appl Physiol* 16:355–360.
- Endo B. 1966. Experimental studies on the mechanical significance of the form of the human facial skeleton. *J Faculty Sci Univ Tokyo* 3:1–101.
- Evans F. 1973. Preservation effects. In: Evans F, editor. *Mechanical properties of bone*. Springfield, IL: Charles C. Thomas. p 56–60.
- Hylander WL. 1987. Loading patterns and jaw movements during mastication in *Macaca fascicularis*: a bone-strain, electromyographic, and cineradiographic analysis. *Am J Phys Anthropol* 72:287–314.
- Hylander WL, Picq PG, Johnson KR. 1991. Masticatory-stress hypotheses and the supraorbital region of primates. *Am J Phys Anthropol* 86:1–36.
- Katz JL, Meunier A. 1987. The elastic anisotropy of bone. *J Biomech* 20:1063–1070.
- Nordsletten L, Kaastad T, Madsen J, Reikeras O. 1994. The development of femoral osteopenia in ovariectomized rats is not reduced by high intensity treadmill training: a mechanical and densitometric study. *Calc Tissue Int* 55:436–442.
- Peterson J, Dechow PC. 2003. Material properties of the human cranial vault and zygoma. *Anat Rec* 274A:785–797.
- Ravosa MJ, Johnson KR, Hylander WL. 2000. Strain in the galago facial skull. *J Morphol* 245:51–66.
- Richmond BG, Wright BW, Grosse I, Dechow PC, Ross CF, Spencer MA, Strait DS. 2005. Finite element analysis in functional morphology. *Anat Rec* 283A:259–274.
- Ross CF. 2001. In vivo function of the craniofacial haft: the interorbital pillar. *Am J Phys Anthropol* 116:108–139.
- Saijo S, Sugimura T. 1993. Dynamic response of the adult monkey maxilla to occlusal forces. *J Osaka Dental Univ* 27:1–22.
- Schwartz-Dabney CL, Dechow PC. 2003. Variations in cortical material properties through the human dentate mandible. *Am J Phys Anthropol* 120:252–277.

- Seipel CM. 1948. Trajectories of the jaws. *Acta Odontol Scandinav* 8:81–191.
- Sicher H, DuBrul L. 1970. *Oral anatomy*, 5th ed. St. Louis, MO: C.V. Mosby.
- Southard KA, Southard TA, Schlechte J, Meis P. 2000. The relationship between the density of the alveolar processes and that of post-cranial bone. *J Dent Res* 79:964–969.
- Strait DS, Wang Q, Dechow PC, Ross CF, Richmond BG, Spencer MA, Patel BA. 2005. Modeling elastic properties in finite element analysis: how much precision is needed to produce an accurate model? *Anat Rec* 283A:275–287.
- Tappen N. 1953. A functional analysis of the facial skeleton with split-line technique. *Am J Phys Anthropol* 11:503–532.
- Tappen N. 1954. A comparative functional analysis of primate skulls by the split-line technique. *Hum Biol* 26:220–238.
- Tappen N. 1957. A comparison of split-line patterns in the skulls of a juvenile and an adult male gorilla. *Am J Phys Anthropol* 15:49–57.
- Wang Q, Dechow PC. 2004. Variations in cortical material properties of baboon mandibles. *Am J Phys Anthropol* 38(Suppl):203.
- Wang Q, Dechow PC. 2006. Elastic properties of external cortical bone in the craniofacial skeleton of the rhesus monkey. *Am J Phys Anthropol* (in press).
- Wang Q, Dechow PC, Wright BW, Ross CF, Strait DS, Richmond BG, Spencer MA. 2006. Surface strain on bone and sutures in a monkey facial skeleton: an in vitro method and its relevance to finite element analysis. In: Vinyard CJ, Ravosa MJ, Wall CE, editors. *Primate craniofacial function and biology*. Springer: New York (in press).
- Weiner S, Traub W, Wagner HD. 1999. Lamellar bone: structure-function relations. *J Struct Biol* 126:241–255.
- Wirtz DC, Schiffers N, Pandorf T, Radermacher K, Weichert D, Forst R. 2000. Critical evaluation of known bone material properties to realize anisotropic FE-simulation of the proximal femur. *J Biomech* 33:1325–1330.
- Zar JH. 1999. *Biostatistical analysis*, 4th ed. Upper Saddle River, NJ: Prentice Hall.
- Zioupou P, Currey D. 1998. Changes in the stiffness, strength, and toughness of human cortical bone with age. *Bone* 22:57–66.